Optical Engineering

SPIEDigitalLibrary.org/oe

Asynchronous indoor positioning system based on visible light communications

Weizhi Zhang
M. I. Sakib Chowdhury
Mohsen Kavehrad

SPIE

Optical Engineering 53(4), 045105 (April 2014)

Asynchronous indoor positioning system based on visible light communications

Weizhi Zhang,* M. I. Sakib Chowdhury, and Mohsen Kavehrad
Department of Electrical Engineering, Pennsylvania State University, University Park, Pennsylvania 16802

Abstract. Indoor positioning has become an attractive research topic within the past two decades. However, no satisfying solution has been found with consideration of both accuracy and system complexity. Recently, research on visible light communications (VLC) offer new opportunities in realizing accurate indoor positioning with relatively simple system configuration. An indoor positioning system based on VLC technology is introduced, with no synchronization requirement on the transmitters. Simulation results show that, with over 95% confidence, the target receiver can be located with an accuracy of 5.9 cm, assuming indirect sunlight exposure and proper installation of light-emitting diode bulbs. [DOI: 10.1117/1.OE.53.4.045105]

Keywords: indoor positioning system; visible light communications; light-emitting diode.

Paper 140049 received Jan. 14, 2014; revised manuscript received Mar. 24, 2014; accepted for publication Mar. 25, 2014; published online Apr. 25, 2014.

1 Introduction

Indoor positioning is a research area that is gaining lots of attention recently. Its applications cover a wide area where the technology can be incorporated into consumer electronics products. For example, in the case of in-house navigation, indoor positioning technology can be utilized by handheld products to provide location identification, and thus guide users inside large museums and shopping malls. Another potential application is location detection of products inside large warehouses where indoor positioning can automate some of the inventory management processes. Indoor positioning techniques, if installed in consumer electronic products, can also be utilized to provide location-based services and advertisements to the users. For the attractive applications mentioned above, many giant corporations are devoting their research and development resources into indoor positioning technologies.

But, rapid positioning indoors are difficult to achieve by global positioning system (GPS) because radio signals from GPS satellites do not penetrate well through walls of large buildings. Hence, users using GPS indoors face large positioning errors as well as not being able to connect to GPS satellites at all. To circumvent this situation, two possible alternatives exist, namely radio frequency (RF)-based techniques and visible light communications (VLC)-based techniques.

RF-based techniques include, but are not limited to, the following technologies: wireless local area network, radio-frequency identification, cellular, ultrawide band, bluetooth,[1–4] etc. These methods deliver positioning accuracies from tens of centimeters to several meters.[5] But this amount of accuracy is not sufficient for the applications described above. Apart from the relatively poor accuracy of indoor positioning achievable by RF-based techniques, they also add to the electro-magnetic (EM) interference. For these reasons, the techniques based on VLC are gaining more attraction.

VLC-based techniques employ fluorescent lamps and light-emitting diodes (LEDs). VLC-based techniques have the advantage that the sources do not produce EM interference, and thus can be used in environments where RF is prohibited. Most of the VLC-based techniques use LEDs as the light source, since they can be modulated more easily compared with fluorescent lamps and hence, location data can be transmitted in a simpler way. Moreover, LEDs are currently being installed in most buildings, especially larger ones, e.g., museums and shopping malls, as the primary lighting source instead of fluorescent lamps since they have the advantage of much longer life and lower operating cost though the initial fixed cost is still higher. So, proposed indoor positioning techniques that are based on VLC and LEDs are excellent options. This article focuses on VLC technology based on LEDs. The accuracy achieved is also better using VLC technology than RF-based techniques as is shown in this article.

There are different positioning algorithms that have been used in the literature and can be broadly divided into three categories: triangulation, scene analysis, and proximity, regardless of the light sources.[6–13] Triangulation is the general name of positioning techniques that use the geometric properties of triangles for location estimation, and consist of mainly two branches: lateration and angulation. Lateration methods estimate the target location by measuring its distances from multiple reference points. In VLC-based positioning techniques, reference points are the light sources and the target is the optical receiver. The distance is measured indirectly by measuring the received signal strength (RSS), time-of-arrival (TOA), or time-difference-of-arrival (TDOA). This article uses RSS-based positioning method as it is found to achieve better accuracy than other methods. Zhou et al. reported an accuracy of 0.5 mm using RSS-based technique.[7] TOA-based methods require complete synchronization among the clocks of transmitters and receiver, and have not been used in VLC-based techniques, but are used for GPS. TDOA-based methods can also be used in

*Address all correspondence to: Weizhi Zhang, E-mail: wuz113@psu.edu

VLC-based systems, while in most cases the TDOA information is acquired indirectly.[8,9] These methods require synchronization among the transmitters.

The second category of triangulation methods, angulation, measure angles relative to several reference points (angle of arrival, AOA). Location estimation is then performed by finding intersection of direction lines, which are radii range from reference points to the target.[10] The widely deployed front-facing cameras, which are inherently imaging receivers, on smartphones and tablets have brought opportunities for this method to become realistic on mobile consumer electronics. However, due to the limited field-of-view (FoV) of these cameras, to reach good performance for a real system, a very dense lighting grid is required; otherwise, the system can only be deployed inside rooms with very high ceilings.

Scene analysis refers to a group of positioning algorithms that matches measured information to a previously calibrated database, thus omitting the computation. TOA, TDOA, RSS, and AOA can be used to collect the measurement data. However, these methods require accurate precalibration for a specific environment and cannot be instantly deployed in a new setting. RSS information is used as the measurement data by Hann et al.[11] and an accuracy of 0.651 cm is reported.

Proximity method is very simple in the sense that it relies only upon a grid of reference points, each having a well-known position; when a target collects signal from a single source, it is considered to be colocated with the source. Thus, the accuracy is no more than the resolution of the grid itself. Lee et al.[12,13] proposed and experimentally demonstrated a proximity-based indoor positioning system, where, apart from positioning provided by the visible light LEDs, a Zigbee wireless network is used to transmit the location information to the observer node, as well as to extend the working range.

As mentioned earlier, this article uses RSS-based triangulation method. One novel aspect of the technique described in this article is that the transmitters do not require synchronization at all, implying no connections are needed among the transmitters. Thus, the system proposed in this article is easier and cheaper to deploy inside different indoor environments.

The rest of the article is organized as follows. Section 2 describes the indoor optical wireless channel, the asynchronous channel multiplexing method, and the positioning method. Section 3 describes the simulation model and includes a signal-to-noise (SNR) analysis and simulation results and discussion on them. Section 4 contains the conclusion of the article.

2 System Design and Positioning Algorithm

2.1 *Indoor Optical Wireless Channel*

As shown in Fig. 1, the system contains a set of LED bulbs on the ceiling and a mobile terminal. LED bulbs function as transmitters, sending different hardware IDs related to their physical locations. An optical receiver inside the mobile terminal extracts the location information to perform positioning.

The optical channels considered in this article are all line-of-sight (LOS) links. Following the research done by Kahn and Barry,[14] the most important quantity to characterize such

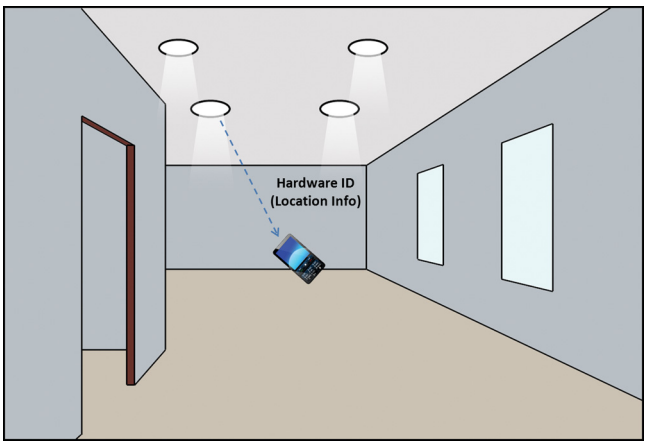

Fig. 1 System configuration.

links is the DC gain. In LOS links, the channel gain can be estimated fairly accurately by considering only the LOS propagation path. The channel DC gain is expressed as

$$H(0)=\begin{cases}\frac{m+1}{2\pi d^2}A\cdot\cos^m(\phi)\cdot T_s(\psi)\cdot g(\psi)\cdot\cos(\psi), & 0\le\psi\le\Psi_c\\ 0, & \psi>\Psi_c\end{cases}, \tag{1}$$

where A is the physical area of the detector, ψ is the angle of incidence with respect to the receiver axis, $T_s(\psi)$ is the gain of optical filter, $g(\psi)$ is the concentrator gain, Ψ_c is the concentrator FoV semi-angle, ϕ is the angle of irradiance with respect to the transmitter perpendicular axis, and d is the distance between transmitter and receiver, as shown in Fig. 2.

The Lambertian order m is given by $m=-\ln 2/\ln(\cos\Phi_{1/2})$, where $\Phi_{1/2}$ is the half power angle of the LED bulb. The received optical power is given by: $P_r=H(0)\cdot P_t$, where P_t denotes the transmitted optical power from the LED bulb.

2.2 *Channel Multiaccess Method*

As shown in Fig. 1, there are multiple transmitters and one receiver in this system. Therefore, the channel multiaccess problem has to be solved. Previous LED-based indoor positioning methods usually use time division multiaccess as a solution, which requires perfect synchronization among all

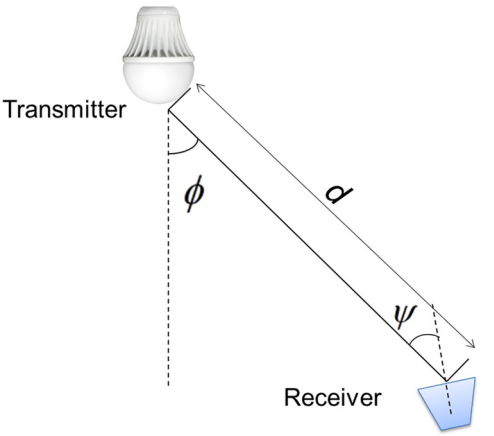

Fig. 2 Channel model.

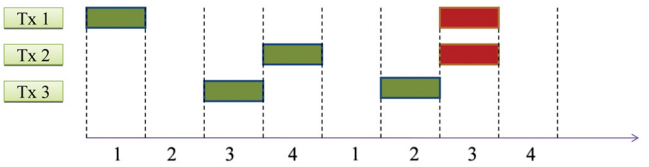

Fig. 3 Basic framed slotted additive link on-line Hawaii system (ALOHA) protocol (three transmitters, four slots per frame).

LEDs, resulting in higher deployment cost and time. Here, an asynchronous channel multiplexing method called basic-framed slotted ALOHA[6,15] (BFSA) is proposed. BFSA is a variant of basic additive link on-line Hawaii system (ALOHA) protocol; it defines a frame structure containing a fixed number of time slots. Each transmitter randomly selects a slot within a frame and transmits its location data in that slot. As each of the transmitters randomly selects a slot, it is possible that sometimes there is overlap among them in time. Such overlap is assumed as a detection failure. Figure 3 shows an example of the working principle of BFSA protocol. There are 3 transmitters and 4 slots and their operation are shown in two frames. In the first frame, the transmitters all select different slots and the receiver will be able to distinguish their signals individually as there is no interference. However, in the second frame, transmitter 1 and 2 both have selected slot 3. Due to this, the receiver will not be able to distinguish their individual signals for their mutual interference and a detection failure is expected in that frame. It should also be noted that since the transmitters are not synchronized, the exact start time of transmission in each slot by the transmitters is different, which may lead to overlap among their transmissions even if they select adjacent slots. Here, detection failure is supposed as a result of any overlap, even partial.

The traditional factor used to evaluate the performance of ALOHA-based protocols is throughput. Throughput is defined as the rate of successful transmission by the nodes. However, it cannot be used in this system for evaluation purposes because the receiver has to receive all signals from different LEDs to estimate its position. In other words, successful reception of only one signal from one transmitter is not enough for the receiver to localize itself. Therefore, the only factor to consider here is the probability of successful transmission from all transmitters to a given receiver.

As mentioned earlier, it is assumed that any overlap among signals will lead to a detection failure. Under this assumption, the probability of successful transmission (P_{success}) in BFSA protocol, given total synchronization, is

$$P_{\text{success}} = \left\langle \begin{matrix} N \\ n \end{matrix} \right\rangle / N^n, \tag{2}$$

where n is the number of transmitters and N is the number of slots in a frame.

When n is bigger than 2, there is no closed mathematical form of P_{success} for asynchronous systems. But difference in performance between synchronous and asynchronous scenarios can be obtained by running computer simulations. Figure 4 shows P_{success} versus the number of slots per frame, N, for four transmitters. It can be seen that when N is large enough (e.g., $N \geq 200$), the performance

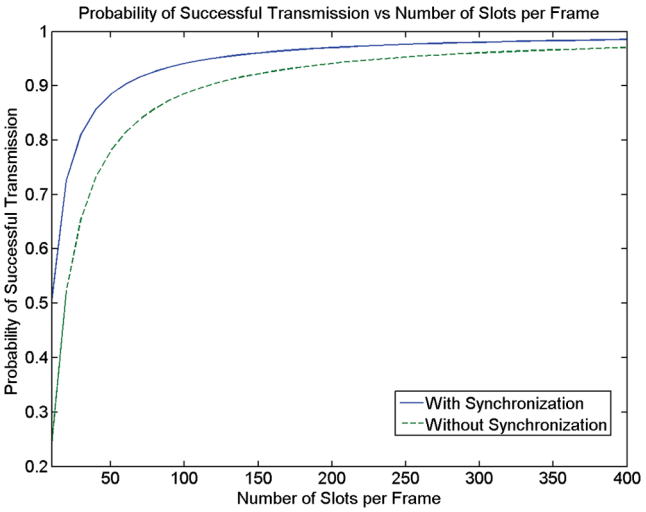

Fig. 4 Probability of successful transmission versus number of slots per frame, $n = 4$.

difference between synchronous and asynchronous systems is negligible.

Now, BFSA protocol requires bandwidth for individual transmitter to be N times of the originally needed. However, the data rate this system is working at is not very high; so, a relatively large N can be chosen to ensure successful transmissions for most of the time.

Suppose 128 bits are used to represent the hardware ID for individual LED bulbs, plus an 8-bit beginning flag, an 8-bit ending flag and a segment of 16-bit CRC to form a packet that is to be transmitted within a frame. The system will perform positioning 10 times per second and use a frame structure containing 400 slots. The required date rate is then given by

$$400 \times (128 + 8 + 8 + 16)\text{bit}/0.1\ \text{s} = 640\ \text{Kbps}. \tag{3}$$

This speed is definitely deliverable even with available off-the-shelf LEDs. On the other hand, with 128 bits the system will be able to label $2^{128} = 3.4 \times 10^{38}$ LEDs, which is far more than actually needed. Therefore, this indoor positioning system will work universally at every place where supporting LEDs are installed.

2.3 *Positioning Algorithm*

In the system, the RSS information of received signal will be used to estimate the receiver's distances from transmitters on the ceiling, after which the receiver will be located by triangulation.

Each of the LED bulbs will simply transmit its own code, modulated in on-off-keying (OOK) format. An LED bulb will use only one slot within the duration of one frame length, while delivering output at a constant power level for illumination purposes. Therefore, the receiver will be receiving only one modulated signal at one instance for most of the time. The OOK modulation used in this system has a modulation depth of 12.5% to minimize the flickering problem.[16] Since the optical emitted power is linearly proportional to the amplitude of the electrical signal, the difference in transmitted power between logical 0s and 1s at the transmitter side is given as

$$P_{\text{diff}} = \eta_{\text{OOK}} P_{\text{const}}, \tag{4}$$

where η_{OOK} is the modulation depth of the OOK modulation and equal to 0.125 in this article.

P_{const} is the optical power emitted from LED bulb without modulation. Therefore, the difference at the receiver side $P_{\text{diff}\,r}$ will be given by

$$P_{\text{diff}\,r} = H(0) \cdot P_{\text{diff}} = \frac{m+1}{2\pi d^2} A \cdot \cos^m(\phi) \cdot T_s(\psi) \cdot g(\psi) \cdot \cos(\psi) \cdot P_{\text{diff}}. \tag{5}$$

Given the receiver's FoV is large enough so that $0 \le \psi \le \Psi_c$ always holds, the distance between the transmitter and the receiver d_{est} can be estimated by measuring $P_{\text{diff}\,r}$ at the receiver:[6]

$$d_{\text{est}} = \sqrt{\frac{(m+1)A \cdot \cos^m(\phi) \cdot T_s(\psi) \cdot g(\psi) \cdot \cos(\psi) \cdot P_{\text{diff}}}{2\pi \cdot P_{\text{diff}\,r}}}. \tag{6}$$

The optical concentrator gain $g(\psi)$ for a compound parabolic concentrator is given as[14]

$$g(\psi) = \begin{cases} \frac{n_C^2}{\sin^2(\Psi_c)}, & 0 \le \psi \le \Psi_c \\ 0, & \psi > \Psi_c \end{cases}, \tag{7}$$

where n_C denotes the refractive index of the concentrator.

Assuming both the receiver axis and the transmitter axis to be perpendicular to the ceiling, the following equations hold:

$$d_{\text{est}} = \sqrt{d_{\text{est}-xy}^2 + H^2}, \tag{8}$$

$$\cos(\phi) = \cos(\psi) = H/d_{\text{est}}, \tag{9}$$

where $d_{\text{est}-xy}$ is the estimated horizontal distance between the transmitter and the receiver and H is the vertical distance between the ceiling and the receiver. All the LEDs are characterized as first-order Lambertian light sources; so, $m = 1$. Also, to simplify the calculation, the transmission of optical filter and the gain of optical concentrator are combined into one gain:

$$T_s(\psi) \cdot g(\psi) = G, \tag{10}$$

where G is a constant related to characteristics of filter and concentrator. Consequently,

$$d_{\text{est}-xy} = \sqrt{\sqrt{\left(\frac{A \cdot G \cdot P_{\text{diff}} \cdot H^2}{\pi \cdot P_{\text{diff}\,r}}\right)} - H^2}. \tag{11}$$

So long as the positions of LEDs related to different codes are known to the receiver, by collecting signals coming from at least three LEDs, the receiver will be able to use triangulation to determine its current position on a two-dimensional plane.

2.4 *Linear Least Square Estimation*

To estimate the unknown position of the receiver by knowing the distances from several reference points (transmitters' horizontal coordinates), linear least square estimation is used since it will provide the most reliable estimation when there are a small number of reference points.

After the estimated horizontal distance between the receiver and each of the three transmitters (denoted as A, B, and C) is obtained, a set of three quadratic equations as follows is formed:

$$(x - x_{\text{A}})^2 + (y - y_{\text{A}})^2 = d_{\text{A}}^2, \tag{12}$$

$$(x - x_{\text{B}})^2 + (y - y_{\text{B}})^2 = d_{\text{B}}^2, \tag{13}$$

$$(x - x_{\text{C}})^2 + (y - y_{\text{C}})^2 = d_{\text{C}}^2, \tag{14}$$

where $[x_{\text{A}}, x_{\text{B}}, x_{\text{C}}]$ and $[y_{\text{A}}, y_{\text{B}}, y_{\text{C}}]$ are the coordinates of LED bulbs in X and Y axes, $[d_A, d_B, d_C]$ are the horizontal distances from the receiver to LED bulbs, (x, y) is the receiver's position to be estimated.

To get one estimation for the receiver's position (x, y), the following equation group has to be solved:

$$\begin{cases} 2x(x_{\text{A}} - x_{\text{C}}) + x_{\text{C}}^2 - x_{\text{A}}^2 + 2y(y_{\text{A}} - y_{\text{C}}) + y_{\text{C}}^2 - y_{\text{A}}^2 = d_{\text{C}}^2 - d_{\text{A}}^2 \\ 2x(x_{\text{B}} - x_{\text{C}}) + x_{\text{C}}^2 - x_{\text{B}}^2 + 2y(y_{\text{B}} - y_{\text{C}}) + y_{\text{C}}^2 - y_{\text{B}}^2 = d_{\text{C}}^2 - d_{\text{B}}^2 \end{cases}. \tag{15}$$

If more than three reference points are involved, all the equation groups formed by any three quadratic equations are first solved, after which the estimations are averaged out to obtain the final estimated position of the receiver.

3 Performance Evaluation

3.1 *Simulation Model*

The system configuration is depicted in Fig. 5. As shown, there are four LED bulbs located on the ceiling. Since the LEDs within one bulb are colocated and modulated by the same circuit, they will perform as a single optical transmitter.

In the proposed system, each of these four LED bulbs will transmit a unique code assigned to them (first four bits are 0111, 1011, 1101, 1110, respectively, the rest 124 bits are same), modulated in OOK format. The receiver is located within the horizontal plane of 1-m height. Parameters used in the simulation are shown in Table 1.

3.2 *SNR Analysis*

Before running the simulation, the SNR is calculated to examine the effects of it on the system. The signal component is given by

$$S = \gamma^2 P_{\text{diff}\,r}^2, \tag{16}$$

where γ is the detector responsivity and $P_{\text{diff}\,r}$ is given by Eq. (5).

Following Komine and Nakagawa's research,[17] the noise is Gaussian having a total variance N, which is the sum of contribution from shot noise and thermal noise, given by

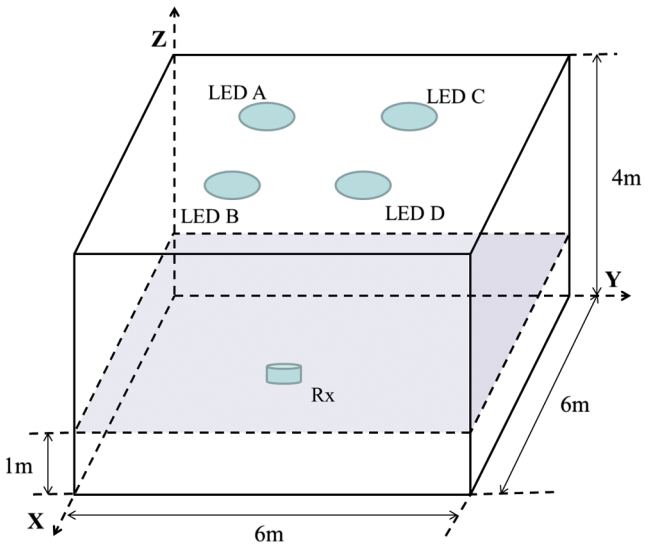

Fig. 5 System model used in simulation.

$$N = \sigma_{\text{shot}}^2 + \sigma_{\text{thermal}}^2. \tag{17}$$

The shot noise variance is given by

$$\sigma_{\text{shot}}^2 = 2q\gamma(P_{\text{rec}})B + 2qI_{bg}I_2B, \tag{18}$$

where q is the electronic charge, B is equivalent noise bandwidth, which is equal to the modulation bandwidth here, I_{bg} is background current, whose traditional value is 5100 μA given direct sunlight exposure and 740 μA assuming indirect sunlight exposure[18] and the noise bandwidth factor, $I_2 = 0.562$.[17] A p-i-n/field-effect transistor (FET) transimpedance receiver is used and the noise contributions from gate leakage current and $1/f$ noise are negligible.[19]

P_{rec} is given by

$$P_{\text{rec}} = \sum_{i=1}^{4} H_i(0)P_i, \tag{19}$$

where $H_i(0)$ and P_i are the channel DC gain and instantaneous emitted power for the i'th LED bulb, respectively.

On the other hand, the thermal noise variance is given by

$$\sigma_{\text{thermal}}^2 = \frac{8\pi kT_K}{G_{\text{o}}}\eta AI_2B^2 + \frac{16\pi^2kT_K\Gamma}{g_m}\eta^2A^2I_3B^3, \tag{20}$$

where the two terms represent feedback-resistor noise and FET channel noise. Here, k is Boltzmann's constant, T_K is absolute temperature, G_{o} is the open-loop voltage gain, η is the fixed capacitance of photodetector per unit area, Γ is the FET channel noise factor, g_m is the FET transconductance, and $I_3 = 0.0868$.

In the simulation, the following values are used:[20] $T_K = 295$ K, $G_{\text{o}} = 10$, $g_m = 30$ mS, $\Gamma = 1.5$, and $\eta = 112$ pF/cm^2. Parameters of the receiver are listed in Table 2. To evaluate the impact of SNR on the system, a distribution map of SNR with respect to LED bulb D, which is located at (4, 4, 4) (m), is shown in Fig. 6, assuming direct sunlight exposure and in Fig. 7, assuming indirect sunlight exposure.

As can be observed from the figures, the SNR is about 10 dB lower in direct sunlight exposed room environment for the same location, compared with indirect sunlight exposure. This is mainly because of the increased contribution from shot noise to the total noise level. Besides, it is shown in both figures that the signal transmitted from LED bulb D experiences a very low SNR at the room corner (0, 0, 0) (m). This will be translated into relatively large error in estimating the distance between the LED bulb D and the receiver when it is located at the corner, in other words, the system performance will be downgraded when the user is far away from the LED bulbs.

Table 1 Parameters in simulation.

Parameter	Value	
Room dimension ($L \times W \times$ H)		$6 \times 6 \times 4$ m^3
Power of light-emitting diode (LED) bulb (P_{const})		16-W each
Positions of LED bulbs (x, y, z) (m)		A(2, 2, 4)
		B(4, 2, 4)
		C(2, 4, 4)
		D(4, 4, 4)
Codes used by LED bulbs	A(0 1 1 1)	(The remaining 124 bits are same)
	B(1 0 1 1)	
	C(1 1 0 1)	
	D(1 1 1 0)	
Modulation depth (η_{OOK})		12.5%
Modulation bandwidth (B)		640 KHz
Receiver height		1 m

3.3 *Results and Discussions*

The system performance is evaluated when the receiver is at a fixed height of 1 m. For the receiver positions, 0.05 m is set as the resolution, meaning that the Euclidean distance between adjacent positions of the receiver is 0.05 m.

Table 2 Receiver parameters.

Parameter	Value
Field-of-view (Ψ_c) (half angle)	70 deg
Physical area of photo-detector (A)	1.0 cm^2
Gain of optical filter ($T_s(\psi)$)	1.0
Refractive index of optical concentrator (n_{C})	1.5
O/E conversion efficiency (γ)	0.54 (A/W)

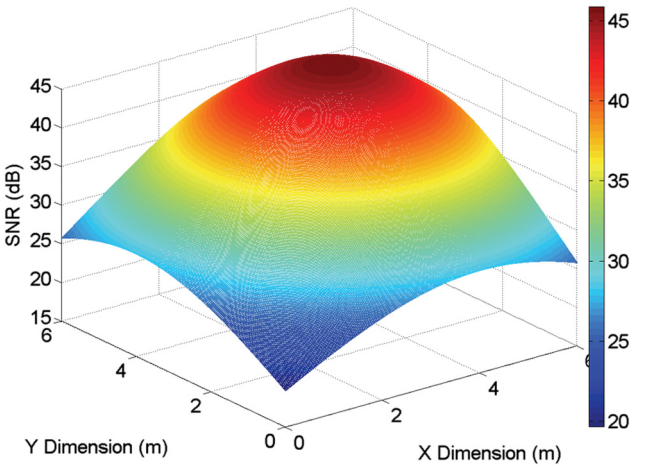

Fig. 6 Signal-to-noise (SNR) distribution for light-emitting diode (LED) bulb D (direct sunlight exposure).

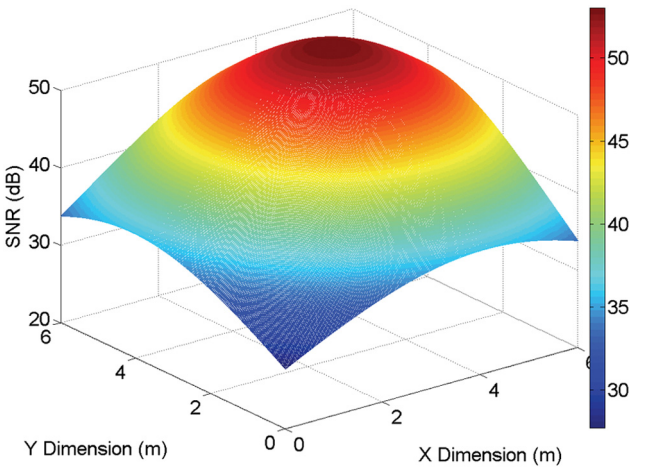

Fig. 7 SNR distribution for LED bulb D (indirect sunlight exposure).

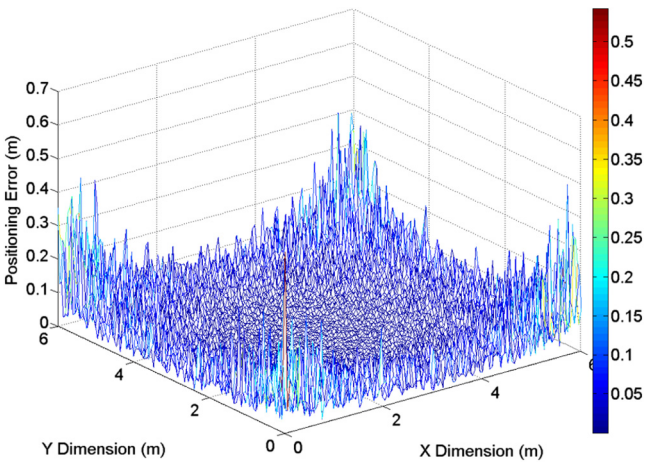

Fig. 8 Positioning error (in units of meter) distribution under direct sunlight exposure.

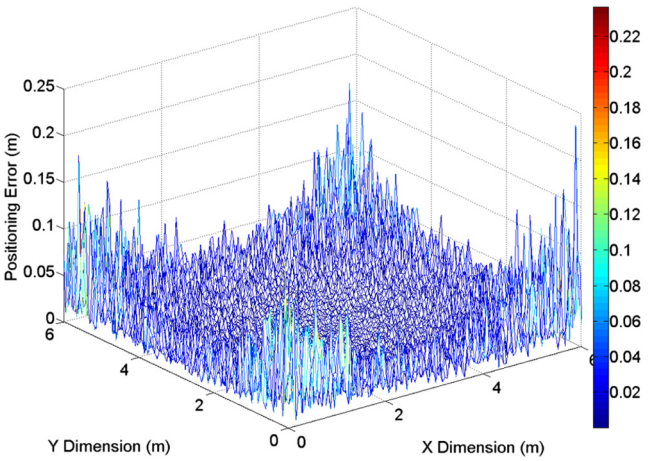

Fig. 9 Positioning error (in units of meter) distribution under indirect sunlight exposure.

Figure 8 shows the positioning error distribution in the presence of direct sunlight exposure and Fig. 9 depicts the result when indirect sunlight exposure is assumed.

As expected, the positioning errors are relatively small for the majority of the room area, but become significantly large when the receiver approaches corners. Moreover, the positioning errors obtained with indirect sunlight exposure are much smaller compared with direct sunlight exposure situation, which is a more noisy environment. To directly compare the difference between these two scenarios, the histograms of positioning errors are shown, respectively, in Figs. 10 and 11.

To assess the performance of a positioning system more practically, precision, which indicates how the system consistently delivers a certain level of service within a long timescale (i.e., over many trials), is widely employed.

Generally, the cumulative distribution function (CDF) of positioning error is used to evaluate the precision. By taking the effects of BFSA protocol into consideration, using a frame structure containing 400 slots per frame for simulation, the precision curve (CDF curve of positioning error) of this system is obtained and shown in Fig. 12.

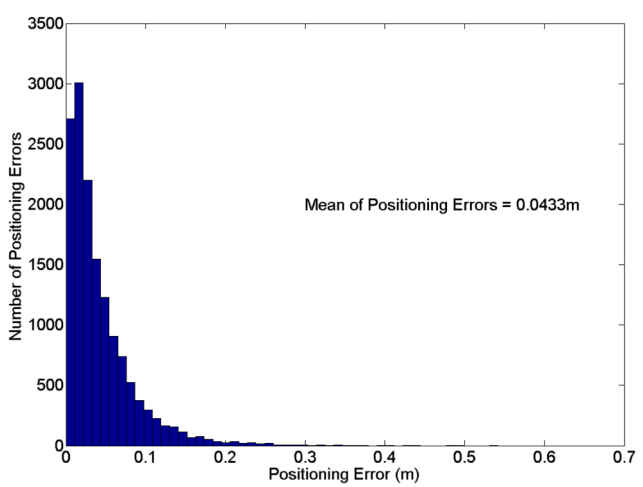

Fig. 10 Histogram of positioning error (direct sunlight exposure).

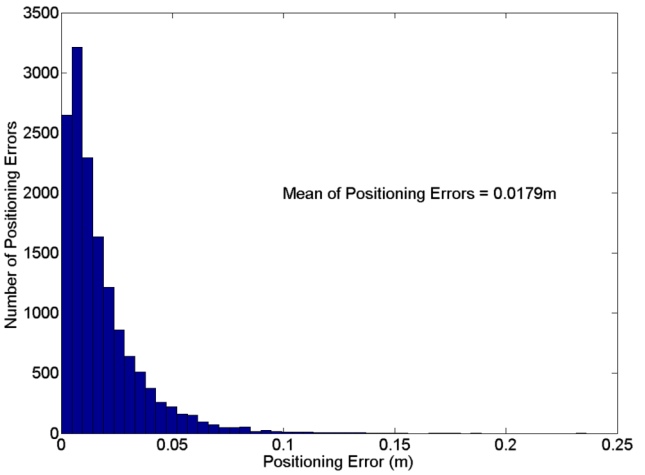

Fig. 11 Histogram of positioning error (indirect sunlight exposure).

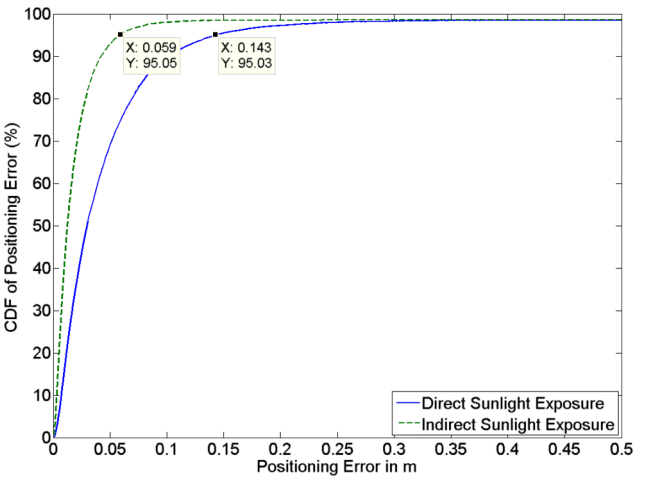

Fig. 12 Cumulative distribution function (CDF) curves of positioning error under direct and indirect sunlight exposure.

As indicated by the curves, if 95% is assumed as an acceptable service coverage rate, the proposed system will be able to deliver an accuracy of 14.3 cm (5.9 cm), within indoor environments with direct (indirect) sunlight exposure.

3.4 *Extended Simulation and Results*

An extended simulation was completed to further evaluate the system performance under realistic conditions, taking wrong positioning of LED bulbs as well as orientation angle of the receiver into consideration. The parameters we used in this extended simulation are shown in Table 3.

Figures 13 and 14 show the positioning error distribution assuming wrong positions of LED bulbs, in the presence of direct and indirect sunlight exposure, respectively. As we can see in these figures, the accuracy of positioning is not severely downgraded due to wrong positioning. This conclusion is confirmed by Figs. 15 and 16, which show the histogram of positioning error under both direct and indirect sunlight exposure.

Table 3 Parameters in extended simulation.

Parameter	Value	
Room dimension ($L \times W \times H$)	$6 \times 6 \times 4$ m^3	
Power of LED bulb (P_{const})	16-W each	
Positions of LED bulbs (x, y, z) (m)	A(2, 2, 4.005)	
	B(3.98, 2, 4)	
	C(2.01, 4.005, 4)	
	D(4, 4.01, 3.99)	
Codes used by LED bulbs	A(0 1 1 1)	(The remaining 124 bits are same)
	B(1 0 1 1)	
	C(1 1 0 1)	
	D(1 1 1 0)	
Modulation depth (η_{OOK})	12.5%	
Modulation bandwidth (B)	640 KHz	
Maximum orientation angle of the receiver	5 deg	
Receiver height	1 m	

As we can see, the mean of positioning errors, in both situations, increases compared with the values shown in Figs. 10 and 11, but not dramatically. Therefore, the performance of this system will remain within the same level, even if the LED bulbs involved are installed at slightly incorrect positions.

The precision curves (CDF curve of positioning error) of this system assuming wrong positions of LED bulbs are shown in Fig. 17. As indicated by the curves, if 95% is assumed as an acceptable service coverage rate, the proposed system will be able to deliver an accuracy of 17.25 cm (11.2 cm), within indoor environments with direct (indirect) sunlight exposure.

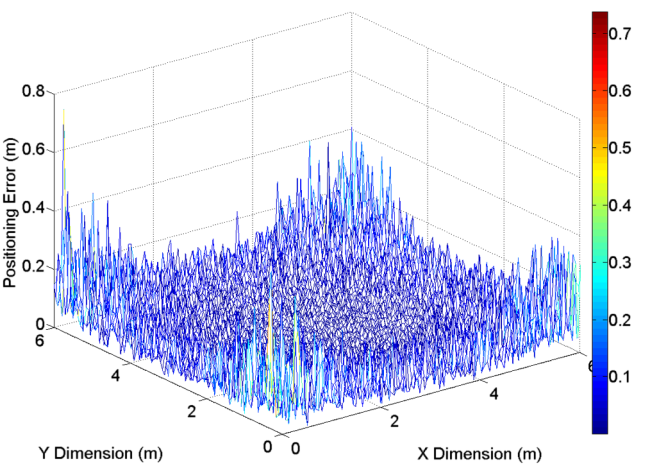

Fig. 13 Positioning error (in units of meter) distribution under direct sunlight exposure assuming wrong positions of LED bulbs.

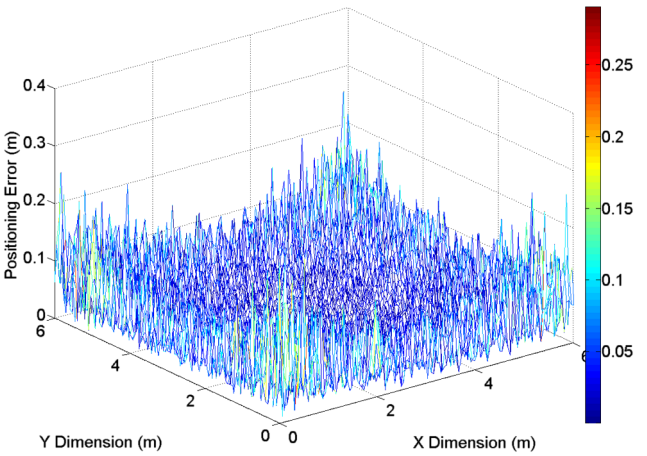

Fig. 14 Positioning error (in units of meter) distribution under indirect sunlight exposure assuming wrong positions of LED bulbs.

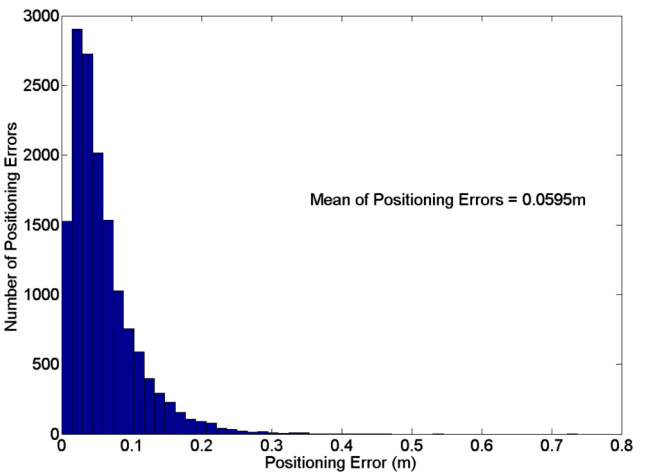

Fig. 15 Histogram of positioning error assuming wrong positions of LED bulbs (direct sunlight exposure).

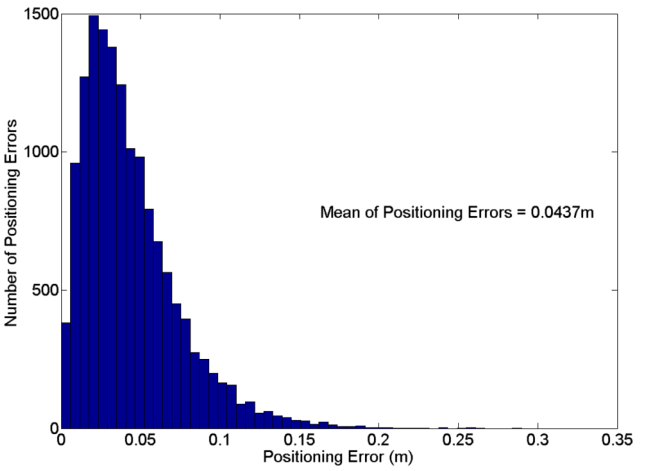

Fig. 16 Histogram of positioning error assuming wrong positions of LED bulbs (indirect sunlight exposure).

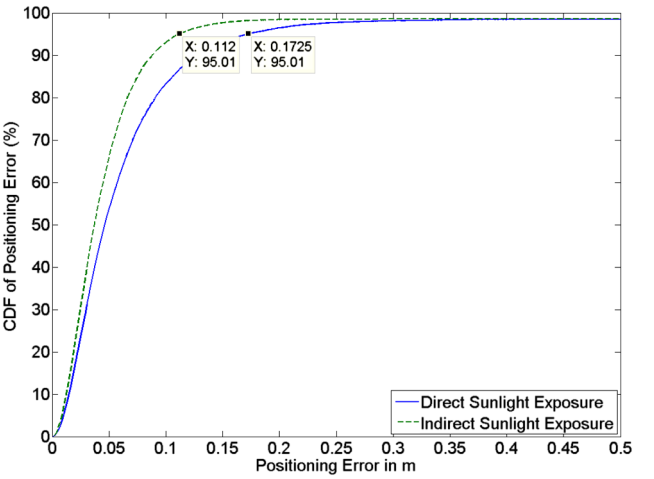

Fig. 17 CDF curves of positioning error under direct and indirect sunlight exposure assuming wrong positions of LED bulbs.

4 Conclusions

In this article, an asynchronous indoor positioning system based on VLC technology is proposed. The use of BFSA protocol is addressed as a solution to the channel multiaccess problem. The feasibility of this protocol is then shown considering the realistic modulation bandwidth of a typical LED. After noise analysis, simulation results for indoor environments with both direct and indirect sunlight exposure were described. Results indicate that the proposed system is able to provide indoor positioning service with a precision of 95% within 17.25 cm assuming direct sunlight exposure, and a precision of 95% within 11.2 cm when indirect sunlight exposure is assumed, taking possible wrong positions of LED bulbs and orientation angle of the receiver into consideration.

Acknowledgments

This research in part was supported by a National Science Foundation award IIP-1169024, IUCRC on optical wireless applications.

References

1. C. Wang et al., "An implementation of positioning system in indoor environment based on active RFID," in *IEEE Joint Conf. on Pervasive Computing*, pp. 71–76 (2009).
2. J. Zhou et al., "Providing location services within a radio cellular network using ellipse propagation model," in *IEEE 19th Int. Conf. Advanced Information Networking and Applications*, pp. 559–564 (2005).
3. Y. Liu and Y. Wang, "A novel positioning method for WLAN based on propagation modeling," in *2010 IEEE Int. Conf. Progress in Informatics and Computing*, pp. 397–401 (2010).
4. L. Son and P. Orten, "Enhancing accuracy performance of Bluetooth positioning," in *2007 IEEE Wireless Communications and Networking Conf.*, pp. 2726–2731 (2007).
5. H. Liu et al., "Survey of wireless indoor positioning techniques and systems," *IEEE Trans. Syst., Man, Cybernet., Part C: Appl. Rev.* **37**(6), 1067–1080 (2007).
6. W. Zhang and M. Kavehrad, "A 2-D indoor localization system based on visible light LED," in *Proc. IEEE Photonics Society Summer Topical Conf.—Optical Wireless Systems Applications*, pp. 80–81 (2012).
7. Z. Zhou, M. Kavehrad, and P. Deng, "Indoor positioning algorithm using light-emitting diode visible light communications," *Opt. Eng.* **51**(8), 085009 (2012).
8. K. Panta and J. Armstrong, "Indoor localisation using white LEDs," *Electron. Lett.* **48**(4), 228–230 (2012).
9. S. Y. Jung, S. Hann, and C. S. Park, "TDOA-based optical wireless indoor localization using LED ceiling lamps," *IEEE Trans. Consum. Electron.* **57**(4), 1592–1597 (2011).

10. T. Tanaka and S. Haruyama, "New position detection method using image sensor and visible light LEDs," in *IEEE Second Int. Conf. Machine Vision. ICMV'09*, pp. 150–153 (2009).
11. S. Hann et al., "White LED ceiling lights positioning systems for optical wireless indoor applications," in *IEEE 36th European Conference and Exhibition on Optical Communication (ECOC)*, pp. 1–3, IEEE (2010).
12. Y. U. Lee et al., "Hybrid positioning with lighting LEDs and Zigbee multihop wireless networks," *Proc. SPIE* **8282**, 82820L (2012).
13. Y. U. Lee and M. Kavehrad, "Two hybrid positioning system design techniques with lighting LEDs and ad-hoc wireless network," *IEEE Trans. Consum. Electron.* **58**(4), 1176–1184 (2012).
14. J. M. Kahn and J. R. Barry, "Wireless infrared communications," *Proc. IEEE* **85**(2), 265–298 (1997).
15. M. Bolic, D. Simplot-Ryl, and I. Stojmenovic, *RFID Systems, Research Trends and Challenges*, Wiley, New York (2010).
16. G. Archenhold, "Health and safety of artificial lighting," *Mondo Arc* **63**, 111–118 (2011).
17. T. Komine and M. Nakagawa, "Fundamental analysis for visible-light communication system using LED lights," *IEEE Trans. Consum. Electron.* **50**(1), 100–107 (2004).
18. A. J. Moreira, R. T. Valadas, and A. M. de Oliveira Duarte, "Optical interference produced by artificial light," *Wireless Networks* **3**(2), 131–140 (1997).
19. R. G. Smith and S. D. Personick, "Receiver design for optical fiber communication systems," in *Semiconductor Devices for Optical Communication*, pp. 89–160, Springer, Berlin Heidelberg (1982).
20. A. P. Tang, J. M. Kahn, and K. P. Ho, "Wireless infrared communication links using multi-beam transmitters and imaging receivers," in *IEEE Int. Conf. Communications. ICC 96, Conference Record, Converging Technologies for Tomorrow's Applications*, Vol. 1, pp. 180–186 (1996).

Weizhi Zhang obtained his BS degree from the Department of Physics at South China University of Technology, Guangzhou, China, in 2009. He is now working toward his PhD degree in electrical engineering at the Pennsylvania State University. He is a researcher at the Center on Optical Wireless Applications (COWA). His research is currently focused on optical communication and related applications, especially indoor optical positioning and free-space optics.

M. I. Sakib Chowdhury obtained his BSc degree in electrical and electronic engineering from Bangladesh University of Engineering and Technology in 2007. He worked for 3 years in the telecommunications industry upon his graduation. He is currently a PhD student in the EE Department at the Pennsylvania State University and a researcher of Center on Optical Wireless Applications (COWA). His research interests include indoor optical wireless communications and radio frequency-based communications in next-generation mobile networks.

Mohsen Kavehrad is with the Pennsylvania State University EE Department as Weiss Chair professor and director of the Center for Information and Communications Technology Research. He has published over 350 papers, book chapters, books, and key patents. His research interests are in the areas of wireless and optical communications networked systems. In January 2012, he became a director of an NSF Industry/University Cooperative Research Center, jointly with Georgia Tech, called the Center on Optical Wireless Applications.